Colloids and Surfaces A: Physicochemical and Engineering Aspects 683 (2024) 132985

Contents lists available at ScienceDirect

Colloids and Surfaces A: Physicochemical and Engineering Aspects

journal homepage: www.elsevier.com/locate/colsurfa

Chemical modification of zeolites for the recovery of rare earth elements evaluated by machine learning algorithms

Óscar Barros [a,b,*], Pier Parpot [a,b], Isabel C. Neves [a,b], Teresa Tavares [a,c]

[a] CEB - Centre of Biological Engineering, University of Minho, Campus de Gualtar, 4710-057 Braga, Portugal
[b] CQUM, Centre of Chemistry, Chemistry Department, University of Minho, Campus de Gualtar, 4710-057, Braga, Portugal
[c] LABBELS – Associate Laboratory, Braga, Guimarães, Portugal

HIGHLIGHTS

- Alkali modifications improved the zeolites natural adsorption capabilities.
- Zeolites had adsorption and desorption with over 80% and 90%, respectively.
- Possible to use unsupervised machine learning algorithms for pattern recognition.
- Supervised machine learning regression models were successfully tested and applied.
- Possible to use classification algorithms to select the best modifications.

GRAPHICAL ABSTRACT

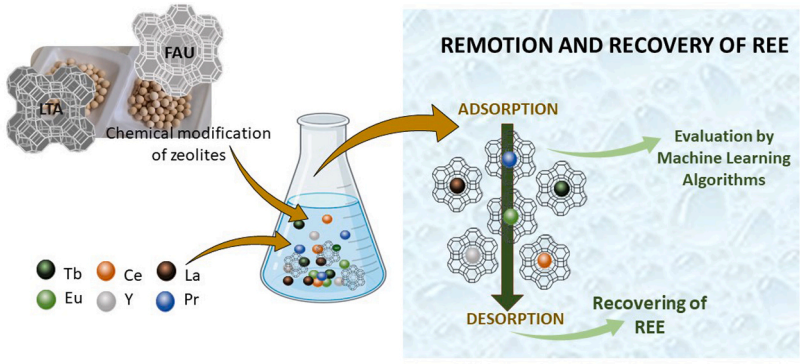

ARTICLE INFO

Keywords:
Zeolite
Rare earth elements
Machine learning
Adsorption
Recovery
Circular economy

ABSTRACT

Rare earth elements (REE) are a significant group of valuable elements used in diverse and relevant applications in our daily lives. The mining and processing of the original ores, as well as the final wastes disposal, produce wastewater with variable concentrations of REE to be recovered. Sorbent materials like zeolites have been employed in adsorption processes to capture diverse pollutants from wastewater. The objective of this study is to identify the most effective modified zeolite for the adsorption and desorption of REE from aqueous solutions. To achieve this, the processes evaluation by machine learning (ML) algorithms was explored through both supervised and unsupervised analyses. The purpose of the usage of such tools was to assist in the selection of the optimal zeolite for REE recovery and to assess the predictive capabilities of the models. Modified zeolites were obtained by acid and alkali treatments in order to increase their sorption capacity compared to the controls and they were characterized by SEM/EDS, FTIR and pH zero point charge. Kinetic modelling and desorption assays were also performed, these last ones to evaluate the REE leaching from the sorbent for the best suitable modified zeolites. An overall removal of 80% for adsorption and over 90% recovery for desorption were achieved for the best modified zeolites. ML algorithms helped to classify the adsorption results and allowed the selection of the

* Corresponding author at: CEB - Centre of Biological Engineering, University of Minho, Campus de Gualtar, 4710-057 Braga, Portugal.
E-mail addresses: oscar.barros@ceb.uminho.pt (Ó. Barros), parpot@quimica.uminho.pt (P. Parpot), ineves@quimica.uminho.pt (I.C. Neves), ttavares@deb.uminho.pt (T. Tavares).

https://doi.org/10.1016/j.colsurfa.2023.132985
Received 27 September 2023; Received in revised form 7 December 2023; Accepted 12 December 2023
Available online 13 December 2023

best suitable modified zeolites. It is concluded that alkali modification of the zeolites surfaces increases their natural adsorption capacity for recovering REE.

1. Introduction

Rare earth elements (REE) are a group of seventeen elements, subdivided into light REE (La to Gd) or heavy REE (Tb to Lu, including Y) [1]. These elements are widely used in various applications due to their specific properties [1,2]. As they are becoming more and more essential, these elements are getting closer attention. REE play a crucial role in advancing various aspects of the materials industry (e.g. catalysis, magnets, metallurgy, information storage, military technologies, transport of energy) [3,4]. In addition, REE offer the remarkable ability to substantially modify material properties even in minute amounts. Consequently, the definition of materials doped with rare earths is now a crucial step in technological advancements. For this reason, several governments and international institutions classified REE as critical materials [1–3]. There is almost no production of REE in European Union (EU) due to the complex exploitation of their deposits [5]. The REE extraction and refining have relevant environmental impact [6], as they are associated with radioactive pollution and toxicity due to the eventual presence of radioactive elements like uranium or thorium [7]. The extraction of REE is associated with technological advancements that emerged in the mid-20th century. During this period, only europium could be industrially extracted on a significant scale, primarily as $EuSO_4$. This is attributed to the fact that europium ions undergo an easier reduction from trivalent to divalent states compared to other REE. The first effective REE isolation technique was developed based on ion exchange chromatography. This technique exploited the differences in stability between different rare-earth citrate chelates. About 1954, another effective method, liquid−liquid extraction, was developed and successfully used in commercial production [8,9]. For that reason, alternative methods to mining for obtaining REE are quite attractive, such as recycling REE from containing waste streams using commercially available materials as zeolites [6]. Some efforts have been made in this context allowing the specific recycling of REE [10] or achieving their recovery and possible reuse [11,12].

Adsorption processes have been extensively used to remove different pollutants from wastewater such as heavy metals [13,14], which led to their recognition as some of the most interesting separation processes. Adsorption is simple and competitive, with high recovery efficiency, with availability of a wide-range of sorbents, effective even with low concentrations of sorbate and environmentally sustainable [1,14–16], making it quite attractive for pollutant removal.

Different inorganic materials are used as sorbents like clays, carbon and zeolites [11,17,18]. Zeolite are crystalline microporous aluminosilicates that are used as catalysts, adsorbents and ion-exchangers [19–21]. Different surface treatments can be used to increase the ion-exchange capacity of the zeolites. The most common modifications on the surface of the zeolites are chemical [22,23] or hydrothermal [24,25] treatments that improve the zeolite porosity. The chemical treatments can be achieved by using mineral salts, alkaline or acidic solutions [26]. These treatments can improve physicochemical properties of the zeolites by the modification of their crystal size, morphology and chemical composition to enhance their adsorption capacity [27]. The acid treatment of zeolites could dissolve some amorphous materials and open the blocked pores of the zeolites [27]. However, this treatment may lead to a dealumination process, which results in an increase of the Si/Al ratio [28]. The alkaline treatment can attack silica, remove silicon ions and increase their mesoporosity, leading to an improvement of the ion exchange ability of the modified zeolite [29]. Briefly, the hydrothermal treatment consists in using an aqueous solution, as an alkali solution, leading to an ion exchange capacity improvement of the zeolite with low Si/Al [30].

Machine learning (ML) models have been recognized as an important tool for wastewater treatment [31,32] in the case of adsorption of antibiotics [33], organic compounds [34] and metals [35,36]. Also, it have been applied to REE separation techniques [37] and to adsorption [38]. In this work, the evaluation by ML algorithms was explored through both supervised and unsupervised analyses. Supervised learning involves the use of labelled data and provides a dataset with features or characteristics and labels [39], and can be divided in classification and regression. Classification is used with discrete labels, when the y values have fixed categorical outcomes, presented by whole numbers designed as integers. It is usual to try more than one algorithm, as KNN, Decision Tree, Random Forest and Logistic Regression, which are widely applied as learning algorithms, adequate to be used for small number of data and their hyperparameters are easily optimized [32]. The unsupervised learning uses data with no labels, aims to explore the data and to find similarities between them [39] and try to find "hidden" labels within the data. For that, clustering and dimensionality reduction algorithms were used. The clustering algorithms consist of a classification method of objects into different groups [39], as K-Means Analysis. The dimensionality reduction aims to remove irrelevant and redundant data to improve data quality and to promote more efficient strategies [39], as Principal Component Analysis (PCA).

This work aims to assess the effect of chemical treatments on different zeolites structures as faujasite (FAU) and Linde Type A (LTA) to improve their sorption capacity for REE entrapment. Acid and alkali treatments with different concentrations were used to modify zeolites. The best chemical treatments were then selected in accordance with the results obtained for the REE adsorption-desorption and kinetics modeling. Furthermore, the adsorption results were analyzed by supervised and unsupervised machine learning.

2. Materials and methods

2.1. Materials

Stock solutions of each rare earth were prepared from the dissolution of the respective salt in distilled water (H_2O) to obtain a solution with a concentration of 1000 mg/L and then used on the batch assays: europium ($EuCl_3.6\ H_2O$; 99.9%) and cerium, ($Ce(NO_3)_3.6\ H_2O$; 99.5%) were purchased from Acros Organics; lanthanum, ($La(NO_3)_3.6\ H_2O$; 99.9%), praseodymium, ($PrCl_3.xH_2O$; 99.9%), terbium, ($TbCl_3.6\ H_2O$; 99.9%) and yttrium, ($YCl_3.xH_2O$; 99.9%) were purchased from Alfa Aesar. The REE used in this work have ionic radii between 1.17 to 1.04 Å due to their different oxidation state, trivalent [40], while their hydrated radii ranged from 2.60 to 2.38 Å, considering the higher hydration coordination, nonahydrates [41]. The multi-element ICP quality control standard solution, with a concentration of each element of 200 mg/L, was purchased from CPAchem. Two zeolite structures were used, FAU (13X) and LTA (4A), typical adsorbents supplied from Acros Organics and Sigma-Aldrich, respectively. The particle size for 13X beads is 4 to 8 mesh with an average pore size of 7.4 Å, while 4A pellets have a diameter of 1.6 mm with an average pore size of 4 Å.

2.2. Zeolite modifications

The 13X and 4A zeolites modifications were carried out on flow columns using different basic and acid solutions. NaOH and KOH at concentrations of 0.10, 0.25 and 0.50 M were used and HNO_3, HCl and H_2SO_4 were tested at a concentration of 0.25 M. The procedure was divided into two steps. In the first step, 20 g of zeolite were washed with 500 mL H_2O for 6 h with a flow rate of 23 mL/min. In the second step,

Table 1
Description of the modification of each tested zeolite with the respective name.

Designation	Modification description
Z13X	zeolite 13X - control
ZX_H2O	zeolite 13X washed with H_2O - control
ZX_NaOH 0.10 M	zeolite 13X modified by NaOH at 0.10 M
ZX_NaOH 0.25 M	zeolite 13X modified by NaOH at 0.25 M
ZX_NaOH 0.50 M	zeolite 13X modified by NaOH at 0.50 M
ZX_KOH 0.10 M	zeolite 13X modified by KOH at 0.10 M
ZX_KOH 0.25 M	zeolite 13X modified by KOH at 0.25 M
ZX_KOH 0.50 M	zeolite 13X modified by KOH at 0.50 M
ZX_HCl 0.25 M	zeolite 13X modified by HCl at 0.25 M
ZX_HNO3 0.25 M	zeolite 13X modified by HNO_3 at 0.25 M
ZX_H2SO4 0.25 M	zeolite 13X modified by H_2SO_4 at 0.25 M
Z4A	zeolite 4A - control
ZA_H2O	zeolite 4A washed with H_2O - control
ZA_NaOH 0.10 M	zeolite 4A modified by NaOH at 0.10 M
ZA_NaOH 0.25 M	zeolite 4A modified by NaOH at 0.25 M
ZA_NaOH 0.50 M	zeolite 4A modified by NaOH at 0.50 M
ZA_KOH 0.10 M	zeolite 4A modified by KOH at 0.10 M
ZA_KOH 0.25 M	zeolite 4A modified by KOH at 0.25 M
ZA_KOH 0.50 M	zeolite 4A modified by KOH at 0.50 M

500 mL of the acid or of base solutions were used for 22 h with a flow rate of 3 mL/min. The resulting modified zeolites will be identified with the respective pre-treatment and concentration. Control of the pre-treatment process was also performed. The control zeolites were designated as ZX_H_2O or ZA_H_2O and were produced by replacing the 500 mL of the pre-treatment second step with H_2O. After this procedure, the zeolites were dried at 60 °C for 48 h before characterization or adsorption-desorption assays. A list of the designation for each sample that will be tested and a description of the chemical modifications performed is shown in Table 1.

2.3. Characterization

The modified zeolites were characterized by Scanning Electron Microscopy/Energy Dispersive X-Ray spectroscopy (SEM-EDS), Fourier-transform infrared spectroscopy (FTIR) and pH_{ZPC}. The characterization procedures by SEM-EDS and pH_{ZPC} were performed similarly to the one reported by Barros *et al.* [11].

FTIR measurements were performed on different samples using an attenuated total reflectance, ATR-FTIR, PerkinElmer Spectrum Two spectrometer equipped with an ATR accessory. A diamond prism was used as the waveguide. Firstly, the samples were reduced to powder and then all spectra were recorded with a resolution of 2 cm^{-1} in the wavelength region 4000–400 cm^{-1} by averaging 50 scans and the analyses were carried out at room temperature.

2.4. Analytical quantification of REE

All liquid samples were analyzed at the Inductively Coupled Plasma - Optical Emission Spectrometry, ICP-OES, (Optima 8000, PerkinElmer). The procedure was very similar to the one reported by Barros *et al.* [11]. This analysis was performed with slightly different operating conditions, namely, RF power at 1400 W, argon plasma flow at 12 L/min, auxiliary gas flow at 0.2 L/min, and nebulizer gas flow at 0.70 L/min. The wavelengths (nm) used for each element were: La—408.672, Ce—413.764, Eu—381.967, Y—371.029, Tb—350.917 and Pr—390.844, with an axial plasma view for La, Ce, Tb and Pr, while for Y and Eu, a radial view was used.

2.5. Selection of modified zeolite by adsorption assays

2.5.1. Adsorption assays

The adsorption assays were carried out using a concentration of 6 g/L of the modified zeolites with a mixed REE solution with a concentration of 10 mg/L of each REE tested. The uptake assays were carried out at room temperature in batch vessels placed in rotary shakers at 130 rpm for 24 h. The same procedure was used in kinetics assays that lasted 125 h. The pH was controlled and the desired values ranged between 3 and 4. When pH was higher than 4, a drop of a diluted solution of HCl would be added. The uptake at a given time for each REE is the mass of such element that is retained per mass of sorbent.

Table 2
The binary classification for the different REE. The C/C_0 values were given a classification accordantly. The mean value of these intervals was taken and given the respective binary classification.

C/C_0 intervals	C/C_0 Classification	Binary Classification
$0.8 < C/C_0 < 1.0$	1	1 if the mean of the classification for the tested REE is above 4.0
$0.6 < C/C_0 < 0.8$	2	
$0.4 < C/C_0 < 0.6$	3	
$0.2 < C/C_0 < 0.4$	4	0 if the mean is below 4.0
$0.0 < C/C_0 < 0.2$	5	

2.5.2. Kinetics modeling

The kinetics modeling was performed using the non-linear forms of the Pseudo-first order (PFO) [42], Eq. (1), and of the Pseudo-second order (PSO) [43] models, Eq. (2). The use of non-linear equations aims to avoid some errors associated with the linearization of the models by changing the error structure or altering their distribution, possibly distorting the fitting as referenced in the literature [44,45].

This fitting was performed using the non-linear equations of both models and the least-squares regression method, using Origin Pro 8.5 software. The equations used are the following:

$$q_t = q_e * (1 - e^{-k_1 * t}) \quad (1)$$

$$q_t = \frac{k_2 * q^2 * e^t}{1 + k_2 * q_e * t} \quad (2)$$

where q_t (mg/g) is the mass of solute retained per mass of solid at time, t; q_e (mg/g) is the mass of adsorbate per unit mass of adsorbent at equilibrium; k_1 is a rate constant (min^{-1}) and reflects a combination of the rate constants of adsorption k_a and desorption k_d; k_2 (g/(mg × min)) is a complex parameter related to the initial concentration of solute.

2.6. Desorption assays

Desorption assays were carried out using 3 different acid solutions: HNO_3, H_2SO_4 and HCl, at a concentration of 0.10 M each in H_2O. The zeolites loaded with REE produced previously were used in these tests.

The assays were carried out at room temperature in rotary shakers at 120 rpm, for 5 h, using a volume of 0.1 L of leaching solution and 0.35 g of loaded zeolite. Samples of the solution were taken and then analyzed by ICP.

The recovery percentage (% recovery) [46] was calculated using Eq. (3):

$$\%recovery = \frac{C_t * V_t}{m_{REE}} \quad (3)$$

where C_t is the concentration of one REE (mg/L) at a given time, V_t is the solution volume (L) of a given time, and m_{REE} is the total mass (g) of a given REE retained by a given zeolite.

2.7. Machine learning

The ML analysis was performed using a table with the C/C_0 results

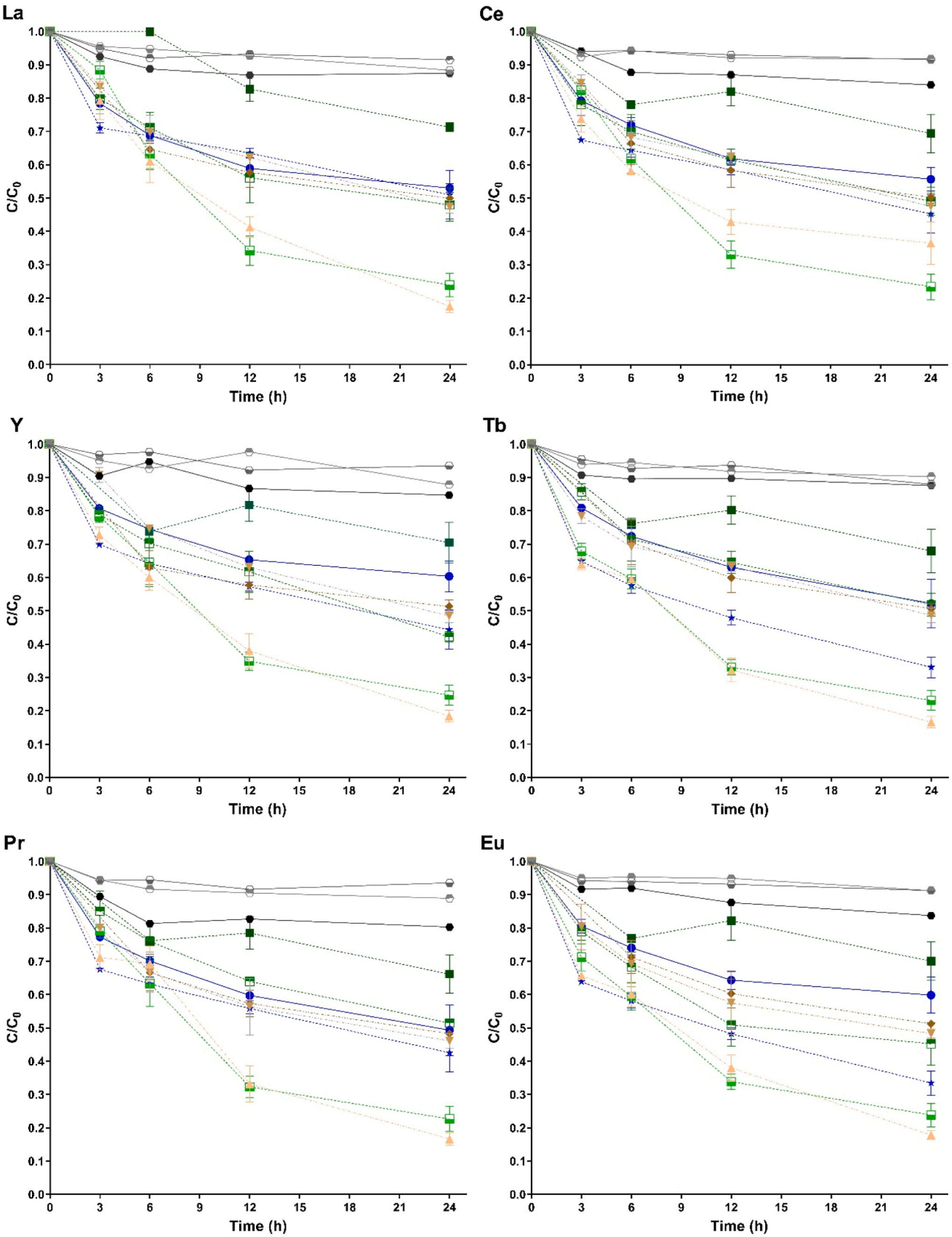

Fig. 1. : REE adsorption on zeolite 13X and modified samples. The assays were carried out with a multi solution of REE previously described. The treated with acid modifications are ZX_HNO3 0.25 M (—○—), ZX_HCl 0.25 M (—⬡—) and ZX_H_2SO_4 0.25 M (—⬢—). The zeolites with alkali modifications are ZX_NaOH 0.1 M (- -△- -), ZX_NaOH 0.25 M (- -▽- -), ZX_NaOH 0.5 M (- -◆- -), ZX_KOH 0.1 M (- -▭- -), ZX_KOH 0.25 M (- -▬- -) and ZX_KOH 0.5 M (- -■- -). The control zeolites are ZX_H_2O (—●—) and Z13X (- -★- -).

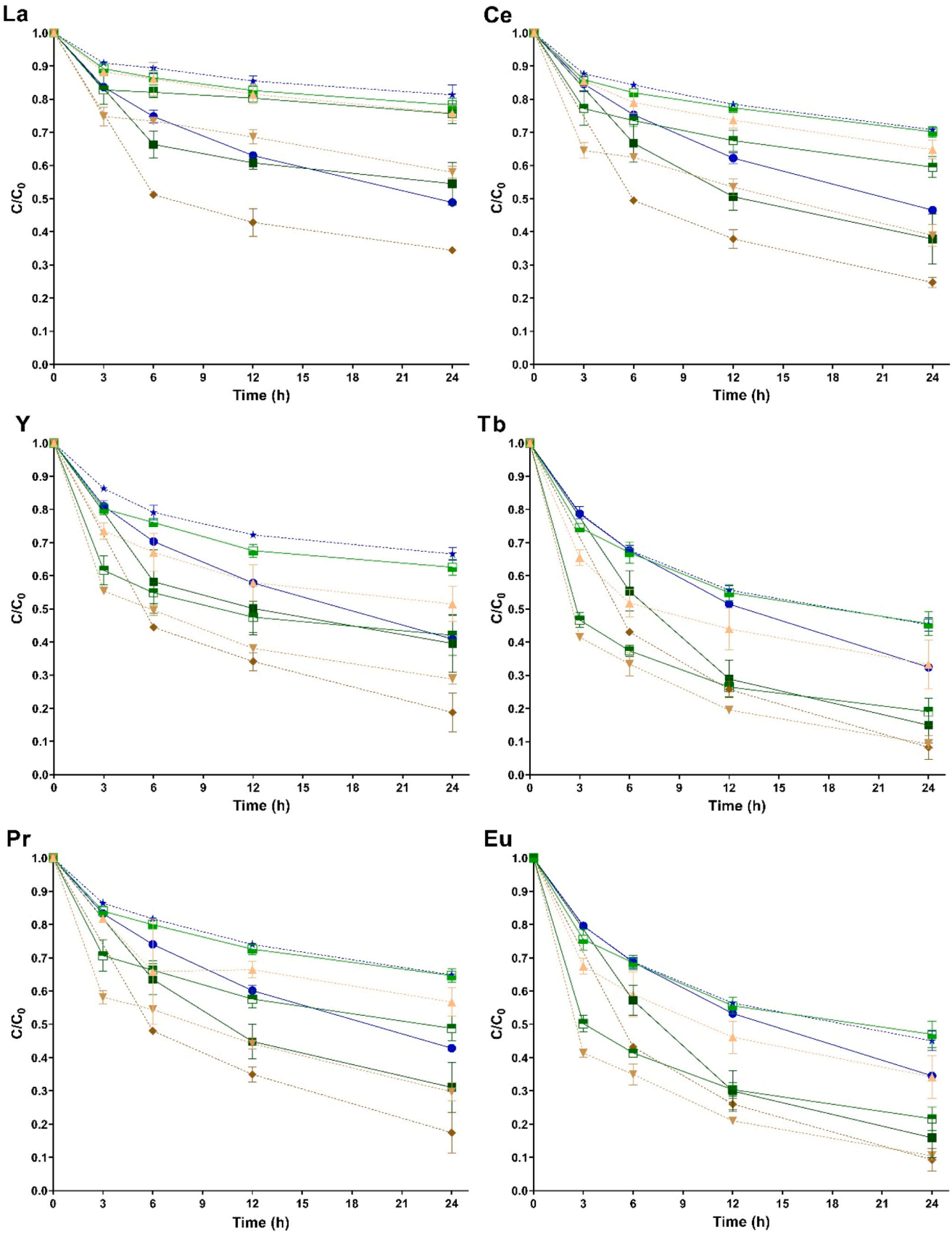

Fig. 2. : REE adsorption on zeolite 4 A and modified zeolites, without pH adjustment. The assays were carried out with a multi solution of REE previously described. The zeolites with alkali modifications are ZA_NaOH 0.1 M (▲), ZA_NaOH 0.25 M (▼), ZA_NaOH 0.5 M (◆), ZA_KOH 0.1 M (□), ZA_KOH 0.25 M (□) and ZA_KOH 0.5 M (■). The control zeolites are ZA_H_2O(●) and Z4A (★).

after 24 h for each tested REE, the pH of the zeolite treatment, pH of the adsorption solution after the 24 h time point for each sample. The resulting table was studied under unsupervised learner (Principal Component Analysis, K-Means Analysis) and supervised learner (classification and regression).

K-nearest neighbors Classifier (KNN), Decision Tree Classifier and Random Forest Classifier were used to classify the samples. These classifiers are often used in binary classification, as explained in Table 2. The data was divided into two sets, a training set (70% of the data), to train the model and a test set (30% of the data), where the model's prediction is tested. It also added a stratify option to the data division, allowing both test and train sets to have the same percentage of positive cases (in this case, a good adsorbent) as the complete set.

For the regression, the training test split was 70% for training and 30% for testing. Different metrics were used to evaluate the regression prediction, which are the mean absolute error (MAE), the mean squared error (MSE), the root mean squared error (RMSE) and the R-Squared (R^2). These metrics were used to evaluate the results of the test data. MAE is calculated by the sum of the absolute differences between the real and predicted values of each tested observation and then divided by the number of observations. MSE is calculated by the average sum of the squared difference between the real and the predicted values. Finally, RMSE is the square root of the value obtained from the MSE.

All tests were performed using Spyder (Python 3.9) and the respective needed modules as pandas, numpy, scikit-learn, matplotlib and seaborn.

2.8. Statistical analysis

The adsorption results were analyzed using the One-Way ANOVA, where the obtained values for each pre-treated zeolite and the respective controls were compared between each other. The Two-Way ANOVA was used for the statistical analysis of the desorption results. The Bonferroni's multiple comparison test was used for both data sets.

The ANOVA analyses were performed using the software Graph Pad Prism version 8.0.2 (Graph Pad Software, Inc, San Diego, CA, USA). The results were only considered significantly different when the probability (*p*-value) was lower than 0.05, assuming a 95% confidence interval.

3. Results and discussion

3.1. Modified zeolites characterization

Two different zeolite structures, FAU (13X) and LTA (4A), were subjected to chemical modification with acid and basic solutions at room temperature.

The SEM results (Fig. S1) show that the modification had small effects on the zeolite morphology, which were more noticeable at higher concentrations of the treatment solutions, as expected. However, these results do not give any specific information regarding the modifications and their eventual impact on the surface characteristics or on the zeolite adsorption behavior.

The elementary quantification of the pristine zeolites and the modified ones were evaluated using EDS analysis for zeolite 13 X (Table S1) and for zeolite 4A (Table S2). For zeolite 13X (FAU), the data provided showed that the sodium present in the framework was entirely replaced by protons of the acid solutions and a dealumination was observed, while an opposed effect was observed for the alkali treatments. The treated 4A (LTA) zeolites have similar Si/Al ratios than the ones found for the controls, suggesting that these samples are only slight affected by the treatments.

The alkali treated zeolites have similar pH_{ZPC} to the respective controls, Z13X or Z4A, Fig. S2. Although there is no difference regarding the pH_{ZPC}, a different behavior during the adsorption is noticed. Overall, there was a decrease in the pH_{ZPC} value for the acid treated Z13X, which could be related with the incorporation of the H^+ from the solution into the zeolite, which reduces its natural negative charge.

FTIR spectra (Fig. S3) are very similar between each zeolite type used. The characteristic bands of the zeolite are identified with small shifts for both zeolite structures. These shifts especially in the case of 13X suggest that the pre-treatments had no drastic effect on the pristine zeolite. The Si/Al ratio of the zeolite 13X and of the modified zeolites, (Table S3) was determined by FTIR analysis using the equation 4:

$$x = 3.857 - 0.00621 W_{DR} \quad (5)$$

In here $x = (1 + \mathrm{Si/Al})^{-1}$ and W_{DR} is the wavenumber at 500–650 cm^{-1}, related to the vibrations of the FAU lattice [47]. The results suggest that the modification affects mainly the most external surface of the zeolite 13X.

3.2. Selection of the most suitable chemical treatment

3.2.1. Selection using adsorption results

The REE ionic radii are small enough, between 1.17 to 1.04 Å [40], so the zeolites Z13X and Z4A are expected to be able to remove those ions from the liquid solution considering their average pore size, 7.4 Å and 4.0 Å, respectively. However, for the Z4A zeolite, it might be harder to remove the REE considering their hydrated radii from 2.60 to 2.38 Å, considering a nonahydrates coordination [41]. The adsorption data from the mixed REE solution with the pre-treated zeolites are presented in Fig. 1.

Overall, independently of the REE, the modified zeolites with alkali treatment showed higher adsorption performance than the acid treated ones. Statistical differences (Table S4) were found for the retention of some REE between the pre-treated sorbents, especially the acid modified zeolites and ZX_KOH 0.50 M, and the controls. As the acid treated 13X zeolite did not show any enhancement of the adsorption ability, it was not considered in the forward experiments. The adsorption process occurs on the material surface and the acid modified zeolites might suffer a reduction of the microporosity and an increase of the mesoporosity, which leads to a reduced surface area and helps to explain the poorer results. The C/C_0 results obtained after the alkali modification of surfaces are similar for both the 0.25 M treatment solutions and for ZX_NaOH 0.50 M when compared to the controls. The ZX_KOH 0.50 M presented worse results, with two significant differences found (Table S4). The samples modified with 0.10 M of NaOH and KOH were the modified zeolites reached the lowest C/C_0 in solution after 24 h, Fig. 1. ZX_NaOH 0.10 M had removals over 80% for five REE, apart from Ce. The results are similar between the controls, Z13X and ZX_H_2O, except for Tb and Eu, for which Z13X presented lower C/C_0, suggesting that the pristine zeolite washing with distilled water does not improve or worsened in terms of adsorption capacity. It should be noticed that the water washing does not change the Si/Al ratio of the zeolite 13X (data not shown). The pH solution was monitored during each of the assays with 13X zeolites, as presented in Fig. S4, and for that, the precipitation of the REE can be discharged for the solutions tested with sorbents treated with alkali with lower concentrations. However, some REE precipitation was observed 3 h after the beginning of the assay with zeolites treated with NaOH or with KOH, 0.50 M. For this reason, the concentration of 0.50 M for both alkali treatment solutions are considered inadequate for the REE recovery.

The REE adsorption tests were also performed with the zeolite 4A and respective modified samples, Fig. 2. It is also shown that one of the controls, Z4A, had the worst results in terms of the different REE adsorption, even with significant differences when compared to the modified zeolites (Table S5). The overall adsorption capacity of the LTA structure increased with the alkali treatments and ZA_NaOH 0.50 M was the best sorbent with removals above 80%, except for La and Ce. The pH monitoring in assays with 4A zeolite is presented in Fig. S5. As with 13 X zeolite, ZA_NaOH 0.50 M and ZA_KOH 0.50 M used in adsorption tests presented some REE precipitation after 3 h of assay.

From data of Fig. 1 and Fig. 2, the uptake, *q*, was calculated after 24 h

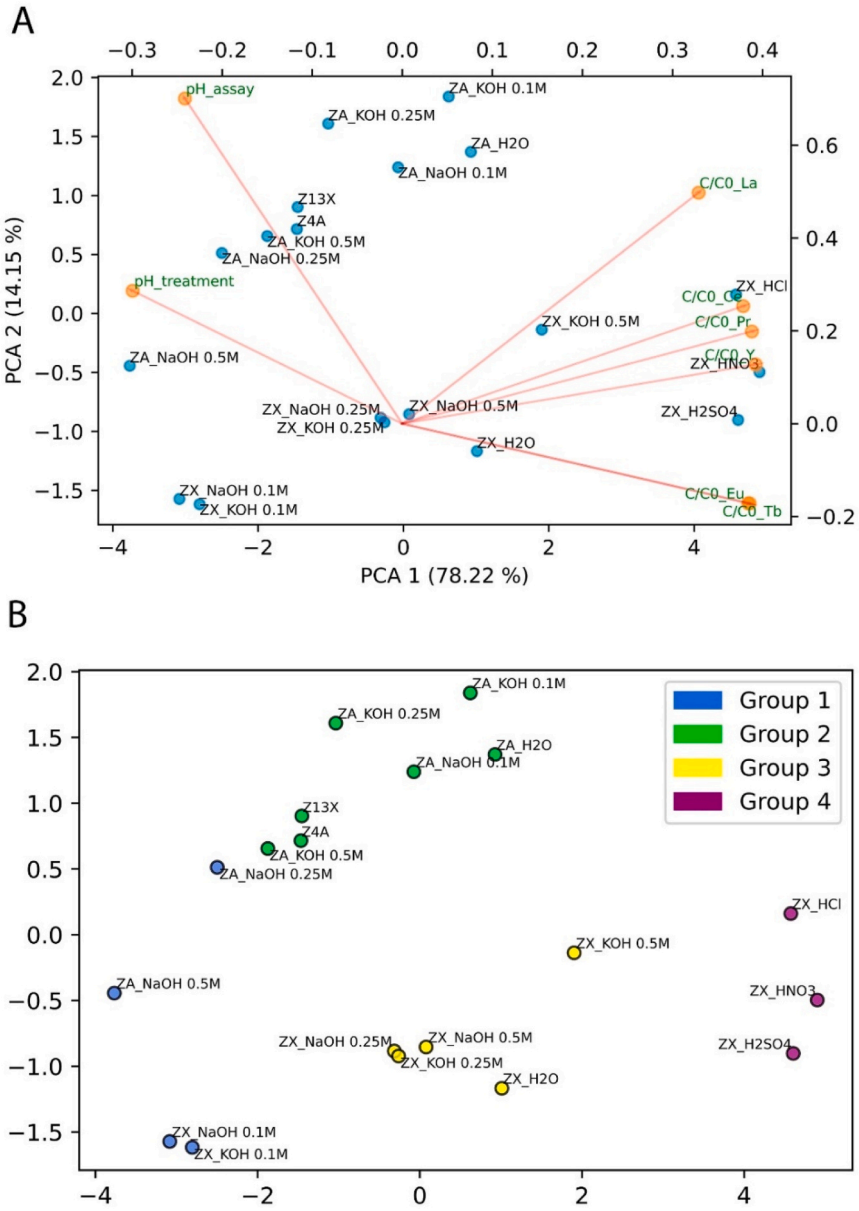

Fig. 3. : Graphical representation ML algorithms analysis of the data obtained at 24 h assay: **A)** PCA analysis and **B)** K-Means algorithm.

of assay. The uptake is defined by the mass of sorbate per mas of sorbent. Its values are presented in Tables S6 and S7 for 13X and 4 A zeolite samples, respectively.

For the zeolite 13X, the ZX_NaOH 0.10 M presented the highest uptake values for most of the REE, except for Y and Pr, suggesting a selective REE adsorption by the zeolite, Table S6. These uptake values are a good indicator that the alkali treatment with the base solution with lowest concentration, improved the adsorption capacity of the zeolite surface. These results confirm that the zeolite structures used in this work have different selectivities toward the cations. LTA show selectivity for small highly hydrated cations as Ag or K. In the case of REE, the selectivity of LTA aims at the small trivalent cations as Y and Pr. In the case of 13X larger trivalent cations as La, Ce and Eu are selected [48].

For the 4A zeolite, the ZA_NaOH 0.5 M had the highest q value (Table S7), except for La. The alkali treatments with NaOH and KOH enhance, in general, better results compared to the ones obtained with the untreated zeolite. The best results were obtained with 0.50 M for both solutions, probably by an improvement in the microporosity of the structure, facilitating the incorporation of the REE into the zeolite matrix.

Comparing ZA_NaOH 0.50 M and ZX_NaOH 0.10 M, (Tables S6 and S7), it is noticeable that the LTA zeolite have the highest q of all tested REE, except for La. The main difference between the LTA and FAU is the way how the β cages are connected. For the LTA, the β cages are linked via oxygen bridges, which form an α cages [49] with small pores of approximately 4.1 Å, while for the FAU, the β cages are linked by double six-membered rings, forming a "supercage" [49] with pores approximately of 7.4 Å. The chemical modification with the alkali solution could explain the differences, since these modifications could lead to alterations in the surface. Considering their ionic radii, between 1.17 to 1.04 Å [40], the REE should easily diffuse into the pores of both LTA and FAU zeolites, however their hydrated radii are higher, between 2.60 to 2.38 Å [41]. The expansion of the ionic radius of REE may impose certain limitations on their ability to penetrate the pores of the LTA. This, associated with the pH solution for the ZA_NaOH 0.50 M remaining between 5.5 to 6.5, in which REE can precipitate, prompted the exclusion of this zeolite in the subsequent sections.

Overall and just from the adsorption results, the zeolites ZX_NaOH

0.10 M and ZX_KOH 0.10 M are the most promising ones to be used in continuous assays. However, it is required to assess their behaviour regarding desorption and the kinetics of both processes.

3.2.2. Sorbents selection evaluated by ML algorithms

The normal analysis of adsorption and desorption results can be laborious and extremely intensive when we are dealing with a large number of information, which could come from different pollutants, methods or sorbents used. For that reason, the development of a ML based analysis can support a faster interpretation of the results with high accuracy giving the best solution for such a problem. Adding to that, with a good characterization of the sorbent, it might help to correlate some of its characteristics with its eventual appropriateness as a sorbent. Finally, in other cases those characteristics can be helpful to foresee the possible design and use of the sorbent for other pollutants. Therefore, employing ML algorithms to choose the most suitable modified zeolite as sorbent in the batch system serves as a preliminary step to assess its application to real conditions in water treatment processes. The selection of the best suitable zeolites was achieved with the classification algorithms, which results were compared with the ones obtained in the adsorption assays. The results obtained from ML algorithms were validated by further experimental adsorption assays. Recently, the same ML tools were used in the selection of the best catalytic system obtained by REE adsorption within zeolites and validated the impact of these new approaches [31]. This analysis used data obtained for each modified zeolite, REE, pH values after 24 h adsorption and the pH_{ZPC} values. The results obtained are shown in Fig. 3.

The process starts with a scaling of the data, followed by a dimension reduction, accordantly to their similarity using a PCA. The selection of the correct number of features to use is required, so that the weight (variance) of each feature contributing to the PCA may be evaluated. It was selected 2 principal components, PCA 1 and PCA 2, were selected as they explain over 92% of the sample variation (Fig. S6A) and confirmed by the Knee locator [50]. The features distribution of the data are seen in Fig. 3**A** that clarifies how they are related to each other, using the *cos* of the angle between the features analyzed and interpreting the resulting values (variables with a coefficient correlation close to 1 are directly proportional, while those close to –1 are inversely related). The coefficient correlation between the pH values of the assay (pH_assay) and those of the treatment pH (pH_treatment) is close to 1, since a higher solution pH of the zeolite chemical treatment should provoke a higher pH during the adsorption assay. Overall, a positive correlation was detected between each REE C/C_0 ratios and the other REE C/C_0 ratios. Nevertheless, when the pH values are correlated with the C/C_0 of the different REE, values closer to –1 are obtained and this shows that as the pH values augment, the values of C/C_0 in the solution decrease.

The weight of the different features on the behaviour of the different modified zeolites is described in Fig. 3**A**. The values of the C/C_0 have high weight on the acid treated 13X zeolite, since for these samples the C/C_0 was still high after 24 h, meaning that there was little or no adsorption. The same happened with ZX_KOH 0.50 M. The zeolites modified with 0.25 M, NaOH 0.50 M and the ZX_H_2O are closer to the center, showing that none of the features have a relatively high influence on the results obtained with those sorbents. On the other hand, the variable pH of the assay has a higher weight on the behavior of the different modified zeolites, 4 A and 13X. For ZA_NaOH 0.50 M and ZA_NaOH 0.25 M, the influence of pH_treatment is higher. The modified zeolites 13X NaOH and KOH 0.10 M are in the opposite position of the C/C_0 values, which could be associated with the improved performance that these modified zeolites during the adsorption of REE and therefore, reaching lower C/C_0 values.

The data was then used in an analysis by the K-Means algorithm, presented in Fig. 3**B**, to evaluate the number of groups that the zeolite samples can be divided into. The correct number of groups, which was 4, shown in Fig. S6B**,** was confirmed using the Knee Locator. Group 4, in purple, shown in Fig. 3**B**, contains the acid treated zeolites, indicating that these treatments are not the most suitable to improve the adsorption capacity of zeolites due to high correlation with C/C_0 ratios, as previously suggested by the results shown in Fig. 1. Group 1, highlighted in blue, includes the 13X modified zeolites with NaOH and KOH 0.10 M and the 4 A modified with NaOH 0.25 M and 0.50 M. This group is situated in the opposite side of the C/C_0, which as previously mentioned is translated into lower C/C_0. In consequence, the zeolites with the best adsorption performance, ZX_NaOH 0.10 M and ZX_KOH 0.10 M (Fig. 1), and the ZA_NaOH 0.50 M (Fig. 2) are included in this group. The only unexpected presence in this group is the ZA_NaOH 0.25 M, since it was not included in the group of the best zeolites in the adsorption analysis. However, the ZA_NaOH 0.25 M was the second best zeolite in terms of q values (Table S7). Group 2, shown in green, includes the others Z4A modified zeolites and Z13X. Group 3, in yellow, has the remaining zeolites 13X. These groups include materials with middle-term adsorption performance, especially zeolites 13X, between a bad performance corresponding to group 4 and a good performance belonging to group 1. The presence of the Z13X in the group dominated by the zeolite 4 A indicate that, for these features, the Z13X is more similar to the zeolite 4A than initially thought.

After an assessment of the experimental data using the PCA and K-Means algorithms, the possibility of the modified zeolites classification was verified. Therefore, it was attributed to each sample a binary classification, where 0 is considered bad or low REE adsorption and 1 is considered a good performance or high REE adsorption, which was made in agreement with Table 2.

The classification was performed using 3 different classifiers: KNN, Decision Tree and Random Forest, to evaluate its sustainability by using ML. The classification will help to select suitable new materials for REE removal from wastewater using zeolites as adsorbents and might be implemented for other pollutants removal to determine the best approach. The zeolites that had a good classification (binary classification of 1) were ZX_KOH and ZX_NaOH 0.1 M and ZA_NaOH 0.25 and 0.5 M. The results of this classification are shown in Fig. S7.

The selection of the best suitable number of neighbors (n_neighbors) by the KNN Classifier, is shown in Fig. S6C, from which 1 neighbor is selected depending on the accuracy values for both training and test sets. The accuracy for the precision, recall and f1-score for each classifier used and for both test and training sets. The precision of one classifier is related to the accuracy of making good predictions, which was 100% for every classifier, being the same values for the recall, value of the correctly identified positive predictions, and f1-score, harmonic mean of the precision and the recall.

In these approaches, it should be noticed that having 100% accuracy on the training sets with a relatively low value for the test set might mean that overfitting occurs for the training set, which is not the best-case scenario. That is, since the idea of the training set is to get a better generalization of the results, then the model is used for unseen data, a test set, which serves to evaluate the capacity of the model to classify the new data. All classifiers presented a 100% score for the training set, shown in Table S8. For the test sets, the results are shown using the precision, recall and f1-scores of the prediction done by the model, considering the actual classification. These results were confirmed by the confusion matrix, Fig. S8, that confirms that there were only true positives (the model predict it is a good adsorbent and it is) and true negatives (the model predict it is a bad adsorbent and it is) values identified.

Overall, this study shows that it is possible to use ML algorithms to support the selection of the best suitable zeolite for the removal of REE. The models used were able to select the best adsorbents in the list with very good metric results.

For the leaching and adsorption kinetics, the selected modified zeolites are ZX_NaOH 0.10 M and ZX_KOH 0.10 M. The ZA_NaOH 0.5 M zeolite will not be considered by the same reasons explained in the previous chapter, while the ZA_NaOH 0.25 M did not have outstanding results during the adsorption that justify its use.

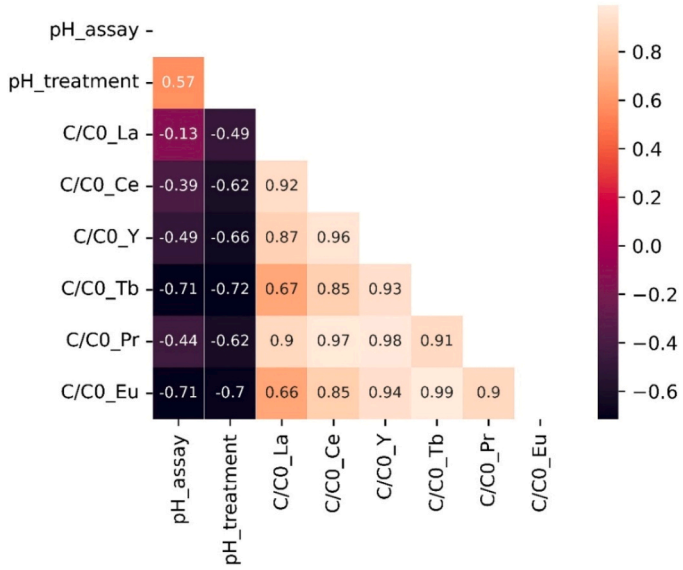

Fig. 4. : Heatmap representing the Pearson correlation between the different features considered in these assays. The left scale represents the different correlation values and the respective colors.

3.2.3. *Predicting unseen data using ML algorithms*

The Pearson correlation was calculated to study the possible correlation and the results are displayed in a heatmap, Fig. 4.

It may be seen that the different pH values (pH_assay and pH_treatment) have a moderate positive correlation (between 0.50 and 0.70) [51]. The pH_assay have a negligible correlation (between 0.00 and -0.30) [51] with the C/C_0 for La, a low negative correlation (between -0.30 and - 0.5) [51] with the results for Ce, Y and Pr and a high negative correlation (between −0.70 and −0.90) [51] with the adsorption of Tb and Eu. With this it would be expected that C/C_0 would be lower as the pH increases till a certain degree (pH values that do not lead to REE precipitation) and this was verified during the adsorption assays. The pH_treatment had moderate negative correlation (between - 0.50 and - 0.70) with the adsorption of Ce, Y and Pr, a high negative correlation (between −0.70 and −0.90) [51] with Tb and Eu and a low negative correlation (between - 0.30 and - 0.5) with La, following the same explanation as before. The C/C_0 correlation between the REE is high (between 0.70 and 0.90) or very high positive (between 0.70 to 0.90) [51], with 2 exceptions: between La and Tb, 0.67, and between La and Eu, 0.66, which are moderate positive correlations. These results suggest that the entrapment values of the REE have a direct correlation with each other, meaning that for the samples used in this study it could be possible to predict the final C/C_0 of one REE using the known values of another REE. It is essential to mention that the correlation is stronger for REE of the same group (light or heavy REE). Pr presented the best correlation with the other tested REE, with values over 0.9, as shown in Fig. 4. This leads to the possibility of only using Pr to estimate the values of other REE present in the solution, considering all zeolites tested and that the results after 24 h assay. The results for the tested linear regressions are shown in Table S9.

Table S9 displayed different metrics used to evaluate the scoring of the estimation of the C/C_0 of the other REE, once the Pr values are known. The lower the values for these metrics, the closer are predicted values to the real ones, indicating that the model predictions are good. The R^2 value is also essential, as it validates a good fitting to the data. As shown, the values are higher than 0.77 for both test and training sets, which is good since it reveals a strong correlation. It may be concluded from the overall metrics evaluated that it is possible to determine the residual REE concentrations in solution, just knowing one of them.

Nevertheless, the REE concentrations prediction was tested for a time period using the data obtained with a single zeolite. Two different adsorption periods were considered, 125 h and 24 h, for the ZX_NaOH 0.10 M. As before, a Pearson correlation was made for the different results of the REE C/C_0, as shown in Fig. 5.

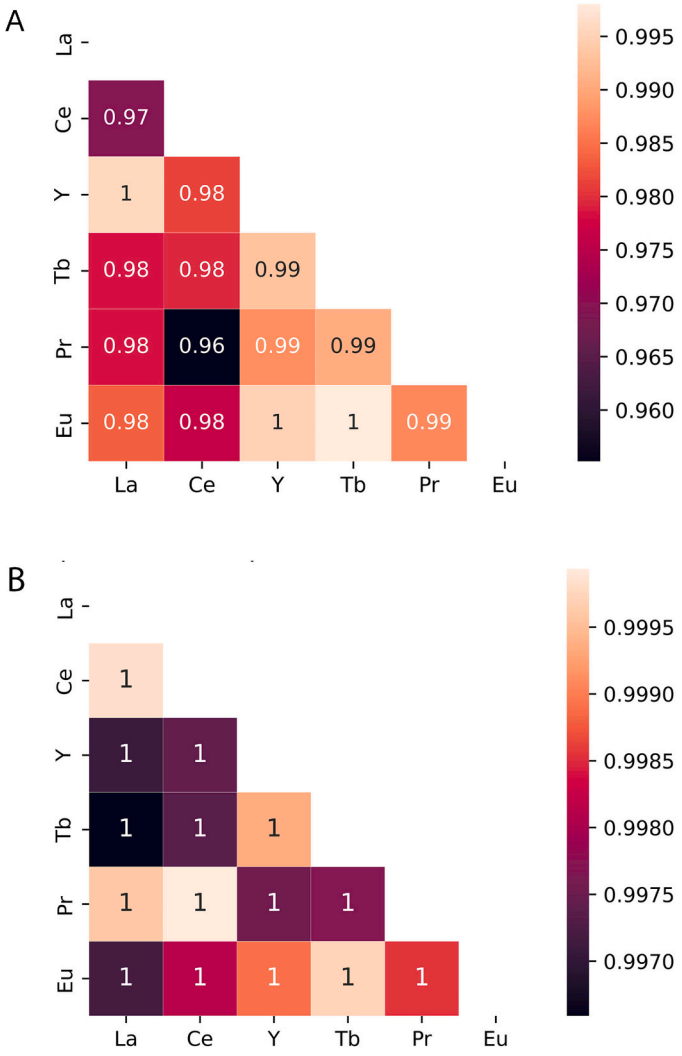

Fig. 5. : Heatmap representation of the Pearson correlations for the different REE after 24 h of contact with the sorbent(**A**) and after 125 h (**B**). The left scale represents the different correlation values and the respective colors.

Fig. 5**A** shows the correlations of the C/C_0 for the different REE for the 24 h adsorption period. The correlation values shown are very high for every REE, including the correlation values obtained with Y, with values above 0.98. In this test, the Y will be used as the *x* value, with the results shown in Table S10. The correlation values for the 125 h assay, shown in Fig. 5**B**, are all for every tested combination. Pr was used as the *x* value and the results are shown in Table S11. When the Pearson Correlation values are compared between the 2 assays, the more extended adsorption test presents a better correlation between the tested REE. That is translated into better metrics and scorings for the models when performing the tests. The methodology was the same as the one performed for the estimation of the C/C_0 values of the zeolite.

The results are much better for the model that used the 125 h adsorption data, since the predicted values are closer to the actual values obtained, showing that increasing the number of data points is essential to construct a good model. For the sake of robustness validation, it was decided to use the model obtained from the 125 h assay to predict the C/C_0 values of the REE in the 24 h assay. The C/C_0 values of Pr were used as *x*, while the rest of the REE values of C/C_0 were predicted from the

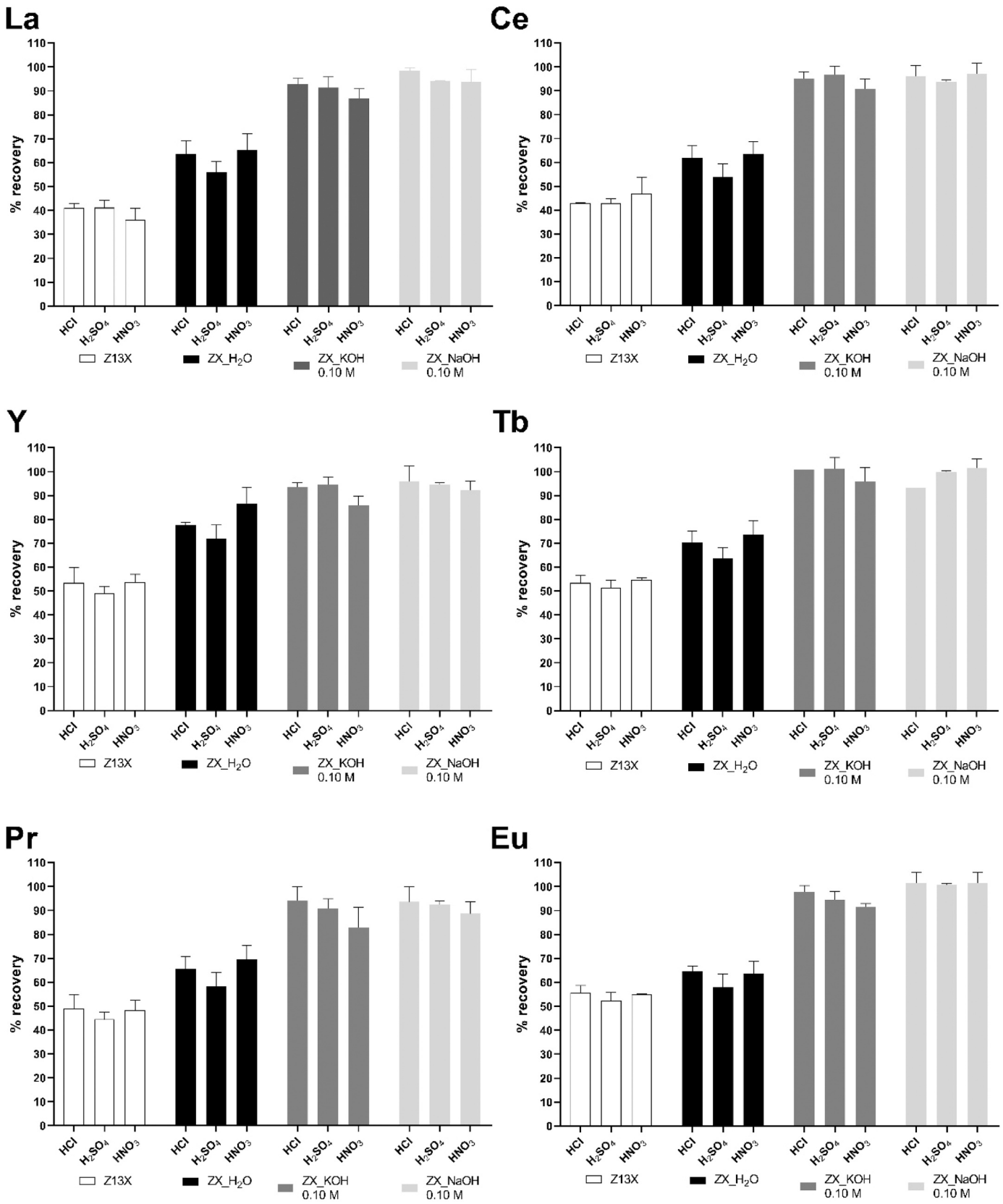

Fig. 6. : Recovery results for Z13X and respective controls with HCl, H_2SO_4 and HNO_3.

previously mentioned model. The metrics and respective scorings between the predicted and actual values are shown in Table S12.

The metrics values in Table S12 are low, showing that the predicted results are very similar to those obtained experimentally. However, comparing these metrics to the ones presented in Table S10 it may be concluded that the model improved with the predictions based on the 125 h assay, with a better prediction capacity.

It is demonstrated that it is possible to predict the final REE C/C_0 in solution, based on the same values for one of the sorbates, as well as to predict the REE C/C_0 values along time, based on those values measured at one time point. The previous work shows that it is possible to train and test a model with a robust prediction capacity and reduced associated errors. These models can be further improved and tested to ensure the best possible prediction. In the future, these models could be an excellent help for faster quantification of metal pollutants, REE or heavy metals, eventually some other pollutants. This could make the quantification of various contaminants in water resources more effortless and faster, leading to quicker treatment.

3.3. Recovery of REE

The selected modified zeolites prepared by alkali treatments were used for the evaluation of leaching processes. HCl, H_2SO_4 and HNO_3 solutions, 0.10 M, were used as eluents. The loaded zeolites were subjected to leaching for 0.5 h and circa 80 to 90% of the entrapped REE were recovered by the liquid solution. This period of contact is the needed to achieve relevant recovery rates of the tested REE while avoiding any damage to the adsorbent. The recovery results for 0.5 h leaching are shown in Fig. 6 for zeolite 13X.

Water leaching REE recovery (data not shown) from both zeolite structures was 5% lower the recovery with acid solutions. This suggests that the presence of H^+ in the solution is required to enhance the removal of the REE from the zeolite eventually by a cationic exchange with the REE^{3+}.

Fig. 6 shows that the zeolites modified with NaOH and KOH 0.10 M had the best recovery, with values near the 100% for all the tested REE. They differ 40 to 45% from the Z13X and 20 to 35% from the ZX_H_2O. A statistical analysis of the recovery values was performed and the results are shown in Table S13. A significant difference for every REE and eluent was observed when comparing with the control Z13X and with the modified zeolites (NaOH or KOH 0.10 M). In addition, a significant difference was also found for most of the REE and eluents tested when comparing the referred recoveries with the ones obtained with the ZX_H_2O control. As expected, comparing the recovery results obtained with the zeolites treated with NaOH or KOH 0.10 M, no significant difference was observed, Fig. 6, but some differences are seen between the controls ZX_H_2O with Z13X. In general, it may be concluded that the alkali treatments improve the REE removal and recovery capacity of zeolites from wastewater.

The tested eluents led to similar recoveries and present no significant difference between them. Therefore, for future assays, the selected eluent will be HNO_3 since this acid is weaker than the others and does not represent an environmental threat as the other ones.

The following step would be a purification process. This process complexity will be dependent of its final objective, presence of other metals, precipitant used and foreseen application for the REE. Some examples described in the literature include the precipitation with carbonate [52], phosphate [53], sulfate [54] and oxalate [55].

3.4. Adsorption kinetics

The selected modified zeolites and the respective controls were used in kinetics evaluations to understand the mechanism of the whole process and its dependence on pre-treatments. Two fitting models were tested: the pseudo first-order, PFO, and the pseudo second-order, PSO. PFO exhibited a better fit to the experimental data compared to PSO (Table S14), attributed to its higher R2 value and the close resemblance between the q_e values predicted by the model and those experimentally obtained (Fig. S9). The PFO model assumes that a change of the solute uptake along time is directly proportional to the difference between sorbent saturation and the uptake along time [56]. The fitting parameters are shown in Table 3 and the confidence intervals in Table S15.

Table 3
Fitting parameters for PFO for the modified 13 X zeolites and respective controls.

		ZX_KOH 0.1 M	ZX_NaOH 0.1 M	ZX_H_2O	Z13X
LA	DF	22	22	37	21
	k_1	0.043	0.044	0.062	0.046
	q_e	3.346	3.380	3.245	3.364
	R^2	0.975	0.969	0.962	0.984
CE	DF	21	26	26	21
	k_1	0.063	0.033	0.099	0.059
	q_e	2.813	4.442	3.220	3.747
	R^2	0.951	0.986	0.925	0.983
Y	DF	22	22	37	32
	k_1	0.051	0.045	0.059	0.045
	q_e	2.971	2.934	2.809	2.681
	R^2	0.964	0.974	0.958	0.970
TB	DF	26	19	29	23
	k_1	0.046	0.048	0.052	0.032
	q_e	3.231	3.063	3.391	3.211
	R^2	0.962	0.967	0.970	0.945
PR	DF	17	26	30	23
	k_1	0.056	0.040	0.075	0.042
	q_e	2.822	3.094	2.753	2.823
	R^2	0.982	0.985	0.977	0.962
EU	DF	19	20	30	20
	k_1	0.056	0.044	0.055	0.029
	q_e	3.011	3.824	3.773	3.939
	R^2	0.969	0.980	0.962	0.949

DF — degrees of freedom; q_e — adsorption capacity at equilibrium calculated from the fitting (mg/g); k_1 — affinity constant of the pseudo-first order model (min^{-1}); R^2 — coefficient correlation.

The q_e values are the theoretical capacity of the zeolite to retain REE at equilibrium, where the highest ones were obtained with ZX_NaOH 0.10 M. This corroborates that for this zeolite, the alkali treatment increased the REE retention as demonstrated before. The k_1 is related to the time required for the interaction between the REE and the zeolite, with both modified zeolites presenting similar values.

The kinetic parameters for REE adsorption by ZX_NaOH 0.10 M were compared with the ones obtained with other inorganic materials [11,17,18] and the results are shown in Table S16. ZX_NaOH 0.10 M has one of the highest q_e values among the considered sorbents and the kinetic parameters indicate a faster interaction of that modified zeolite with the REE in solution. The ratio between the different REE concentrations and the adsorbent concentration certainly determine the differences noticed.

4. Conclusions

It is shown that zeolites are able to remove REE from aqueous solution defining a method for recovering REE from wastewater. The REE adsorption capacities of the FAU (13X) and LTA (4A) zeolites were enhanced after the alkali treatment, being the best results obtained with 0.10 M NaOH for 13X and with 0.50 M NaOH for 4A. The application of both supervised and unsupervised machine learning algorithms proved to be successful in the selection of the most effective modified zeolite, as well as predicting unseen data. The best recoveries for the desorption were obtained after 0.5 h, with no leaching of REE with water as eluent. A significant recovery improvement was detected when comparing the modified and the pristine zeolites. HNO_3 at 0.10 M was selected to work as eluent for further assays as it induces good recoveries and is a weaker acid when compared to the others tested. The FAU modified with NaOH 0.10 M (ZX_NaOH 0.10 M) presented the best fitting parameters in terms of the tested kinetic models, showing an overall improvement in both capacity and rate compared to the untreated zeolites. Further

exploration and development of the ML models can be undertaken by incorporating additional critical features, expanding the dataset, and adjusting algorithm parameters. This approach aims to enhance the understanding of the process and, consequently, to refine the model.

CRediT authorship contribution statement

Tavares Teresa: Conceptualization, Supervision, Validation, Writing – review & editing. **Neves Isabel Correia:** Conceptualization, Supervision, Validation, Writing – review & editing. **Barros Óscar:** Conceptualization, Data curation, Formal analysis, Investigation, Software, Writing – original draft. **Parpot Pier:** Software, Validation, Writing – review & editing.

Declaration of Competing Interest

The authors declare that they have no known competing financial interests or personal relationships that could have appeared to influence the work reported in this paper.

Data Availability

Data will be made available on request.

Acknowledgments

O. Barros thanks FCT for the concession of his Ph.D. grant (SFRH/BD/140362/2018). This study was supported by the Portuguese Foundation for Science and Technology (FCT) under the scope of the strategic funding of UID/BIO/04469/2020 and UID/QUI/0686/2020 units and BioTecNorte Operation (NORTE-01-0145-FEDER-000004) funded by the European Regional Development Fund under the scope of Norte2020—Programa Operacional Regional do Norte, Portugal.

Appendix A. Supporting information

Supplementary data associated with this article can be found in the online version at doi:10.1016/j.colsurfa.2023.132985.

References

[1] I. Anastopoulos, A. Bhatnagar, E.C. Lima, Adsorption of rare earth metals: a review of recent literature, J. Mol. Liq. 221 (2016) 954–962, https://doi.org/10.1016/j.molliq.2016.06.076.
[2] F. Zhao, E. Repo, Y. Meng, X. Wang, D. Yin, M. Sillanpää, An EDTA-β-cyclodextrin material for the adsorption of rare earth elements and its application in preconcentration of rare earth elements in seawater, J. Colloid Interface Sci. 465 (2016) 215–224, https://doi.org/10.1016/j.jcis.2015.11.069.
[3] V. Balaram, Rare earth elements: a review of applications, occurrence, exploration, analysis, recycling, and environmental impact, Geosci. Front. 10 (2019) 1285–1303, https://doi.org/10.1016/j.gsf.2018.12.005.
[4] E. Giese, Rare Earth Elements: therapeutic and diagnostic applications in modern medicine, Clin. Med. Rep. 2 (2018), https://doi.org/10.15761/CMR.1000139.
[5] K.M. Goodenough, J. Schilling, E. Jonsson, P. Kalvig, N. Charles, J. Tuduri, E. A. Deady, M. Sadeghi, H. Schiellerup, A. Müller, G. Bertrand, N. Arvanitidis, D. G. Eliopoulos, R.A. Shaw, K. Thrane, N. Keulen, Europe's rare earth element resource potential: an overview of REE metallogenetic provinces and their geodynamic setting, Ore Geol. Rev. 72 (2016) 838–856, https://doi.org/10.1016/j.oregeorev.2015.09.019.
[6] S. Peelman, D. Kooijman, J. Sietsma, Y. Yang, Hydrometallurgical recovery of rare earth elements from mine tailings and WEEE, J. Sustain. Metall. 4 (2018) 367–377, https://doi.org/10.1007/s40831-018-0178-0.
[7] C.E.D. Cardoso, J.C. Almeida, C.B. Lopes, T. Trindade, C. Vale, E. Pereira, Recovery of rare earth elements by carbon-based nanomaterials—a review, Nanomaterials (2019), https://doi.org/10.3390/nano9060814.
[8] C. Piguet, Extricating erbium, 370–370, Nat. Chem. 6 (2014), https://doi.org/10.1038/nchem.1908.
[9] B. Zheng, J. Fan, B. Chen, X. Qin, J. Wang, F. Wang, R. Deng, X. Liu, Rare-Earth doping in nanostructured inorganic materials, Chem. Rev. 122 (2022) 5519–5603, https://doi.org/10.1021/acs.chemrev.1c00644.
[10] R. Otto, A. Wojtalewicz-Kasprzak, Patent. Method for Recovery of Rare Earths from Fluorescent Lamps, USOO8628734B2, 2014. ⟨https://patents.google.com/patent/US7976798B2/en⟩ (accessed April 24, 2019).
[11] Ó. Barros, L. Costa, F. Costa, A. Lago, V. Rocha, Z. Vipotnik, B. Silva, T. Tavares, Recovery of Rare Earth Elements from wastewater towards a circular economy, Molecules 24 (2019) 1005, https://doi.org/10.3390/molecules24061005.
[12] S.C. Gutiérrez-Gutiérrez, F. Coulon, Y. Jiang, S. Wagland, Rare earth elements and critical metal content of extracted landfilled material and potential recovery opportunities, Waste Manag 42 (2015) 128–136, https://doi.org/10.1016/j.wasman.2015.04.024.
[13] S.Y. Lee, H.J. Choi, Persimmon leaf bio-waste for adsorptive removal of heavy metals from aqueous solution, J. Environ. Manag. 209 (2018) 382–392, https://doi.org/10.1016/j.jenvman.2017.12.080.
[14] T.C. Nguyen, P. Loganathan, T.V. Nguyen, J. Kandasamy, R. Naidu, S. Vigneswaran, Adsorptive removal of five heavy metals from water using blast furnace slag and fly ash, Environ. Sci. Pollut. Res. 25 (2018) 20430–20438, https://doi.org/10.1007/s11356-017-9610-4.
[15] Z. Xi, B. Chen, Removal of polycyclic aromatic hydrocarbons from aqueous solution by raw and modified plant residue materials as biosorbents, J. Environ. Sci. 26 (2014) 737–748, https://doi.org/10.1016/S1001-0742(13)60501-X.
[16] S.M. Yakout, A.A.M. Daifullah, Removal of selected polycyclic aromatic hydrocarbons from aqueous solution onto various adsorbent materials, Desalin. Water Treat. 51 (2013) 6711–6718, https://doi.org/10.1080/19443994.2013.769916.
[17] N. Kano, M. Pang, Y. Deng, H. Imaizumi, Adsorption of rare earth elements (REEs) onto activated carbon modified with potassium permanganate (KMnO4), J. Appl. Solut. Chem. Model. 6 (2017) 51–61, https://doi.org/10.6000/1929-5030.2017.06.02.1.
[18] A.K. Mosai, L. Chimuka, E.M. Cukrowska, I.A. Kotzé, H. Tutu, The recovery of rare earth elements (REEs) from aqueous solutions using natural zeolite and bentonite, Water, Air, Soil Pollut. 230 (2019), 188, https://doi.org/10.1007/s11270-019-4236-4.
[19] B. Silva, H. Figueiredo, C. Quintelas, I.C. Neves, T. Tavares, Zeolites as supports for the biorecovery of hexavalent and trivalent chromium, Microporous Mesoporous Mater. 116 (2008) 555–560, https://doi.org/10.1016/j.micromeso.2008.05.015.
[20] S.M. Al-Jubouri, S.I. Al-Batty, S. Senthilnathan, N. Sihanonth, L. Sanglura, H. Shan, S.M. Holmes, Utilizing Faujasite-type zeolites prepared from waste aluminium foil for competitive ion-exchange to remove heavy metals from simulated wastewater, Desalin. WATER Treat. 231 (2021) 166–181, https://doi.org/10.5004/dwt.2021.27461.
[21] N.H. Ibrahim, S.M. Al-Jubouri, Facile preparation of dual functions zeolite-carbon composite for zinc ion removal from aqueous solutions, Asia-Pac. J. Chem. Eng. (2023), e2967, https://doi.org/10.1002/apj.2967.
[22] B. Silva, H. Figueiredo, O.S.G.P. Soares, M.F.R. Pereira, J.L. Figueiredo, A. E. Lewandowska, M.A. Bañares, I.C. Neves, T. Tavares, Evaluation of ion exchange-modified Y and ZSM5 zeolites in Cr(VI) biosorption and catalytic oxidation of ethyl acetate, Appl. Catal. B Environ. 117–118 (2012) 406–413, https://doi.org/10.1016/j.apcatb.2012.02.002.
[23] A. Martins, V. Neves, J. Moutinho, N. Nunes, A.P. Carvalho, Friedel-Crafts acylation reaction over hierarchical Y zeolite modified through surfactant mediated technology, Microporous Mesoporous Mater. 323 (2021), 111167, https://doi.org/10.1016/j.micromeso.2021.111167.
[24] C. Zou, G. Sha, H. Gu, Y. Huang, G. Niu, Facile solvothermal post-treatment to improve hydrothermal stability of mesoporous SBA-15 zeolite, Chin. J. Catal. 36 (2015) 1350–1357, https://doi.org/10.1016/S1872-2067(15)60857-9.
[25] Q. Qiu, X. Jiang, G. Lv, Z. Chen, S. Lu, M. Ni, J. Yan, X. Deng, Adsorption of heavy metal ions using zeolite materials of municipal solid waste incineration fly ash modified by microwave-assisted hydrothermal treatment, Powder Technol. 335 (2018) 156–163, https://doi.org/10.1016/j.powtec.2018.05.003.
[26] F. Jahani, R. Sadeghi, M. Shakeri, Ultrasonic-assisted chemical modification of a natural clinoptilolite zeolite: enhanced ammonium adsorption rate and resistance to disturbing ions, J. Environ. Chem. Eng. 11 (2023), 110354, https://doi.org/10.1016/j.jece.2023.110354.
[27] A. Filippidis, N. Kantiranis, Experimental neutralization of lake and stream waters from N. Greece using domestic HEU-type rich natural zeolitic material, Desalination 213 (2007) 47–55, https://doi.org/10.1016/j.desal.2006.03.602.
[28] T. Wüst, J. Stolz, T. Armbruster, Partially dealuminated heulandite produced by acidic REECl3 solution: A chemical and single-crystal X-ray study, 84 (1999) 1126–1134. ⟨doi:10.2138/am-1999-7-815⟩.
[29] H. Lin, Q. Liu, Y. Dong, Y. He, L. Wang, Physicochemical properties and mechanism study of clinoptilolite modified by NaOH, Microporous Mesoporous Mater. 218 (2015) 174–179, https://doi.org/10.1016/j.micromeso.2015.07.017.
[30] C. Wang, J. Yu, K. Feng, L. Wang, J. Huang, Synthesis of porous magnetic zeolite-based material and its performance on removal of Cd2+ ion and methylene blue from aqueous solution, Microporous Mesoporous Mater. 345 (2022), 112256, https://doi.org/10.1016/j.micromeso.2022.112256.
[31] Ó. Barros, P. Parpot, E. Rombi, T. Tavares, I.C. Neves, Machine learning approach for classification of REE/Fe-zeolite catalysts for fenton-like reaction, Chem. Eng. Sci. (2023), 119571, https://doi.org/10.1016/j.ces.2023.119571.
[32] G. Alam, I. Ihsanullah, M. Naushad, M. Sillanpää, Applications of artificial intelligence in water treatment for optimization and automation of adsorption processes: recent advances and prospects, Chem. Eng. J. 427 (2022), 130011, https://doi.org/10.1016/j.cej.2021.130011.
[33] A.A. Al-Gheethi, M.S. Mohd Salleh, E.A. Noman, R.M.S.R. Mohamed, R. Crane, R. Hamdan, M. Naushad, Cephalexin adsorption by acidic pretreated jackfruit adsorbent: a Deep Learning prediction model study, Water 14 (2022) 2243, https://doi.org/10.3390/w14142243.
[34] K. Zhang, S. Zhong, H. Zhang, Predicting aqueous adsorption of organic compounds onto biochars, carbon nanotubes, granular activated carbons, and

resins with Machine Learning, Environ. Sci. Technol. 54 (2020) 7008–7018, https://doi.org/10.1021/acs.est.0c02526.
[35] A.H. Sadek, O.M. Fahmy, M. Nasr, M.K. Mostafa, Predicting Cu(II) adsorption from aqueous solutions onto nano zero-valent aluminum (nZVAl) by Machine Learning and Artificial Intelligence techniques, Sustainability 15 (2023) 2081, https://doi.org/10.3390/su15032081.
[36] J. Abdi, G. Mazloom, Machine learning approaches for predicting arsenic adsorption from water using porous metal–organic frameworks, Sci. Rep. 12 (2022), 16458, https://doi.org/10.1038/s41598-022-20762-y.
[37] T. Liu, K.R. Johnson, S. Jansone-Popova, D. Jiang, Advancing rare-earth separation by machine learning, J. Am. Chem. Soc. 2 (2022) 1428–1434, https://doi.org/10.1021/jacsau.2c00122.
[38] G. de V. Brião, D.S.P. Franco, F.V. da Silva, M.G.C. da Silva, M.G.A. Vieira, Critical rare earth metal adsorption onto expanded vermiculite: accurate modeling through response surface methodology and machine learning techniques, Sustain. Chem. Pharm. 31 (2023), 100938, https://doi.org/10.1016/j.scp.2022.100938.
[39] S.N. Dhage, C.K. Raina, A review on machine learning techniques, Int. J. Recent Innov. Trends Comput. Commun. 4 (2016) 395–399. ⟨https://www.researchgate.net/publication/41845861_A_REVIEW_OF_STUDIES_ON_MACHINE_LEARNING_TECHNIQUES⟩. accessed August 11, 2023.
[40] J.H.L. Voncken, Physical and chemical properties of the rare earths. Rare Earth Elem. - An Introd, Springer, Cham, 2016, pp. 53–72, https://doi.org/10.1007/978-3-319-26809-5_3.
[41] W.W. Rudolph, G. Irmer, On the Hydration of the Rare Earth Ions in Aqueous Solution, J. Solut. Chem. 49 (2020) 316–331, https://doi.org/10.1007/s10953-020-00960-w.
[42] S.K. Lagergren, About the theory of so-called adsorption of soluble substances, Sven. Vetensk. Handingarl (24) (1898).
[43] Y.S. Ho, G. McKay, Pseudo-second order model for sorption processes, Process Biochem 34 (1999) 451–465, https://doi.org/10.1016/S0032-9592(98)00112-5.
[44] J. Lin, L. Wang, Comparison between linear and non-linear forms of pseudo-first-order and pseudo-second-order adsorption kinetic models for the removal of methylene blue by activated carbon, Front. Environ. Sci. Eng. China 3 (2009) 320–324, https://doi.org/10.1007/s11783-009-0030-7.
[45] N. Ayawei, A.N. Ebelegi, D. Wankasi, Modelling and Interpretation of Adsorption Isotherms, J. Chem. 2017 (2017) 1–11, https://doi.org/10.1155/2017/3039817.
[46] V. Ajao, K. Nam, P. Chatzopoulos, E. Spruijt, H. Bruning, H. Rijnaarts, H. Temmink, Regeneration and reuse of microbial extracellular polymers immobilised on a bed column for heavy metal recovery, Water Res 171 (2020), 115472, https://doi.org/10.1016/j.watres.2020.115472.
[47] I. Kuźniarska-Biernacka, K. Biernacki, A.L. Magalhães, A.M. Fonseca, I.C. Neves, Catalytic behavior of 1-(2-pyridylazo)-2-naphthol transition metal complexes encapsulated in Y zeolite, J. Catal. 278 (2011) 102–110, https://doi.org/10.1016/j.jcat.2010.11.022.
[48] A. Dyer, Ion-exchange properties of zeolites, in: J. Čejka, H.B.T.-S. in S.S., C. van Bekkum (Eds.), Zeolites Ordered Mesoporous Mater. Prog. Prospect., Elsevier, 2005, pp. 181–204, https://doi.org/10.1016/S0167-2991(05)80011-4.
[49] L.B. McCusker, C. Baerlocher, Chapter 3: Zeolite structures. Stud. Surf. Sci. Catal, Elsevier,, 2001, pp. 37–67, https://doi.org/10.1016/S0167-2991(01)80244-5.
[50] V. Satopaa, J. Albrecht, D. Irwin, B. Raghavan, Finding a "Kneedle" in a haystack: detecting knee points in system behavior, in: 31st Int. Conf. Distrib. Comput. Syst. Work., 2011, IEEE, 2011, pp. 166–171, https://doi.org/10.1109/ICDCSW.2011.20.
[51] M.M. Mukaka, Statistics corner: a guide to appropriate use of correlation coefficient in medical research. Malawi Med. J. 24 (2012) 69–71, accessed July 2, 2023.
[52] P. Kim, A. Anderko, A. Navrotsky, R. Riman, Trends in structure and thermodynamic properties of normal rare earth carbonates and rare earth hydroxycarbonates, Minerals 8 (2018) 106, https://doi.org/10.3390/min8030106.
[53] S. Wu, L. Zhao, L. Wang, X. Huang, Y. Zhang, Z. Feng, D. Cui, Simultaneous recovery of rare earth elements and phosphorus from phosphate rock by phosphoric acid leaching and selective precipitation: Towards green process, J. Rare Earths 37 (2019) 652–658, https://doi.org/10.1016/j.jre.2018.09.012.
[54] K.N. Han, Effect of anions on the solubility of rare earth element-bearing minerals in acids, Min., Metall. Explor. 36 (2019) 215–225, https://doi.org/10.1007/s42461-018-0029-3.
[55] L. He, Q. Xu, W. Li, Q. Dong, W. Sun, One-step separation and recovery of rare earth and iron from NdFeB slurry via phosphoric acid leaching, J. Rare Earths. 40 (2022) 338–344, https://doi.org/10.1016/j.jre.2021.01.003.
[56] T.R. Sahoo, B. Prelot, Adsorption processes for the removal of contaminants from wastewater: the perspective role of nanomaterials and nanotechnology, Nanomater. Detect. Remov. Wastewater Pollut. (2020) 161–222, https://doi.org/10.1016/B978-0-12-818489-9.00007-4.